Optimal Control for Cancer Chemotherapy ODE Models: Potential of Optimal Schedules and Choice of Objective Function

Michael Engelhart

Interdisciplinary Center for Scientific Computing (IWR)
Heidelberg University
Im Neuenheimer Feld 368
69120 Heidelberg, Germany

Dirk Lebiedz

Modeling and Scientific Computing
Zentrum für Biosystemanalyse
Freiburg University
Habsburgerstr. 49
79104 Freiburg, Germany

Sebastian Sager

Interdisciplinary Center for Scientific Computing (IWR), as above

Abstract

In this article, four different mathematical models of chemotherapy from the literature are investigated with respect to optimal control of drug treatment schedules. The various models are based on two different sets of ordinary differential equations and contain either chemotherapy, immunotherapy, anti-angiogenic therapy or combinations of these. Optimal control problem formulations based on these models are proposed, discussed and compared. For different parameter sets, scenarios, and objective functions optimal control problems are solved numerically with Bock's direct multiple shooting method.

In particular, we show that an optimally controlled therapy can be the reason for the difference between a growing and a totally vanishing tumor in comparison to standard treatment schemes and untreated or wrongly treated tumors. Furthermore, we compare different objective functions. Eventually, we show that there is a high potential for optimization of chemotherapy schedules, although the currently available models are not yet appropriate for transferring the optimal therapies into medical practice due to patient-, cancer-, and therapy-specific components.

Keywords:
optimal control, cancer chemotherapy, mathematical modeling, multiple shooting
2010 MSC: 92C50, 92C42, 93C15

1. Introduction

While scientific computing has become an indispensable ingredient of research and every-day-practice in robotics and mechanics, chemical engineering, aerospace, transportation, and many other areas, the application of numerical methods to find answers to open questions in medicine is not yet as evolved.

Scientific computing, and in particular modeling, simulation, and optimization of processes, is often regarded as the third pillar of science, complementary to theory and experiment. In medicine however, experiments are not so easily reproducable as in mechanics, and the theoretic interpretation of drug influence is usually not as well understood as control parameters in physical systems.

Email address:
michael.engelhart@iwr.uni-heidelberg.de (Michael Engelhart)
URL: http://mathopt.uni-hd.de (Michael Engelhart)

There are many different levels on which tumor growth and possible control targets can be modeled. Inherently this is a complex multi-scale problem. A mathematical model can be stochastic or deterministic, spatially resolved or not, continuous or agent-based. Also the level of detail may vary. For example, there may be good reasons to include circadian rhythms and the cell cycle, [1]. A comprehensive overview can be found in the highly recommendable survey paper by Jean Clairambault [2].

We are aware of the fact that the influence of drugs is often not fully understood in medicine, and of course highly patient-dependent (e.g., see the parameter sets "human 9"/"human 10" in [3], respectively [4]). Hence it cannot be expected that currently available models of ordinary differential equations are a good match to clinical reality. A patient- and tumor-specific parameter estimation for well-understood mathematical models based on clinical data will hopefully lead the way and might allow application of optimized treatment schedules in the future.

This work is supposed to be another small step in the direction of analysis and understanding of optimal control chemotherapy models. The basic mathematical models that have been proposed in the literature over the last years (e.g., [3, 5, 6, 7, 8, 9, 10, 11]) should already capture several important dynamic effects of chemotherapy treatments. Having in mind that the gap between simulated and real-world situation will still be large, we focus in this work on general qualitative insight that can be gained by optimization of available mathematical models. Examples for basic questions that are important in this context are

- What similarities and what differences arise for the different mathematical models? We discuss two mathematical models for cancer and cancer chemotherapy. Although they both contain some kind of chemotherapy, they differ in the kind of additional treatments and in type and amount of cell types they include. For the two models, four parameter sets have been described in the literature. We present optimal control results for all of them (see section 5), to the best of our knowledge three sets (see Sections 5.2, 5.3, and 5.4) were not solved to optimality before.

- How large is the potential for the right timing of drug delivery? In general, the aim of a therapy, no matter what kind, is to *minimize* the tumor size, i.e., the tumor volume or the amount of tumor cells. To answer this question, we consider also therapies which, with a fixed amount of drugs, *maximize* the tumor size on a given time horizon. The result, a therapy which makes the tumor grow as big as possible under these constraints, can be considered the *worst* treatment one could apply. We compare these results to standard treatments or untreated tumors as well as the optimal control for a minimal tumor, the *best* treatment. It turns out that there are scenarios where the differences between worst and best treatments are small, but we also demonstrate scenarios where the same amount of drugs leads to a growing tumor on the one hand and a total disappearance on the other hand (see Figures 1, 5, 7, and 9).

- How does the choice of the objective function influence the optimal control strategies? The formulation of a reasonable objective function is crucial for the optimal treatment schedules. We formulate new optimal control problems with non-standard objective functions for models for which such problems have not been published yet, see Sections 5.1, 5.2, 5.3, and 5.4.

- What role do local optima play? As the computational effort do perform a rigorous global optimization for all of the scenarios we considered is beyond the scope of this paper, we concentrated on some case studies with multiple initializations. Whereas for most scenarios the local optima seem to be the unique global ones, also multiple local optima were observed, compare Figure 6 left and right. This effect is closely linked to the choice of the objective function. Including a penalization of tumor volume integrated over time in the objective function seems to favor multiple local optima.

Our approach to address these questions by numerical optimization is based on Bock's direct multiple shooting approach to solve optimal control problems. The underlying *first discretize, then optimize* concept allows for an efficient and fast solution of a multitude of different control problems.

This article is structured as follows. In the next two sections, we review and present the different models (section 2) and control problems (section 3) that have been investigated. Section 4 explains the direct multiple shooting techniques we used to solve the arising optimal control problems. Numerical results can be found in Section 5, where also some interpretations and comparisons between the different scenarios are discussed. We conclude with a summary of our results and an outlook on future work.

2. Cancer Chemotherapy Models

Two different models of cancer chemotherapy with a total of four different parameter sets have been investigated. The models consist of sets of ordinary differential equations and each feature a particular kind of medical treatment. In this section, an overview over the models is given and differences between them are highlighted. We also present their scientific context and give a survey of adjacent approaches we did not consider in detail. In general, we stick to the notation of the original articles if this does not conflict with the overall notation in this article.

2.1. d'Onofrio et al.

The model by *d'Onofrio et al.* [7] is based on the work by *Hahnfeldt et al.* [5] and in particular on a modification of the *Hahnfeldt*-model by *d'Onofrio and Gandolfi* [12, 13].

In [5], a model with two states and one control is proposed. The states are the volume of the tumor x_0 on the one hand and the volume of blood vessels in the neighborhood of the tumor x_1 on the other hand. This choice of state variables is due to the fact that the treatment strategy includes an *anti-angiogenic* therapy u_0 in this model, a concept introduced in the 1970s by *Folkman* [14]. As a tumor needs proliferating blood vessels to survive and to grow, the basic idea is to administer a drug that suppresses *angiogenesis*, the process of blood vessel formation from existing vessels. While the cytostatic agents applied in classical chemotherapy address the proliferation of tumor cells directly, anti-angiogenic drugs inhibit the stimulation of endothelial cells necessary for neo-vascularization.

The tumor volume equation contains a *Gompertz*-term

$$-\zeta\, x_0(t) \log\left(\frac{x_0(t)}{x_1(t)}\right) \tag{1}$$

in which the limit has been replaced by the endothelial volume. *Gompertz growth* beside *logistic growth* is one of the two types of growth chosen in all models that have been investigated. Inserting the blood vessel volume as *carrying capacity* instead of a fixed value reflects that the growth of the tumor is limited by the vasculature volume. In [7] a classical chemotherapy treatment has been added, so that a combination therapy is possible and thus the model contains a second control u_1 representing a cytostatic drug:

$$-F\, x_0(t)\, u_1(t). \tag{2}$$

The equation for the blood vessel volume is more complex. It contains a term that represents the spontaneous loss of vasculature and one that represents the stimulation of *neo-vascularization* by the tumor (e.g., by the cytokine *VEGF, vascular endothelial growth factor*),

$$-\mu\, x_1(t) + b\, x_0(t). \tag{3}$$

The third term,

$$-d\, x_0(t)^{\frac{2}{3}} x_1(t), \tag{4}$$

reflects the effect of endogenous inhibition of angiogenesis. Finally, with

$$-G\, u_0(t)\, x_1(t) - \eta\, x_1(t)\, u_1(t) \tag{5}$$

the response to the drugs is modeled. In contrast to [5], drug concentration is identified with dosage here. Hence, there is no concentration equation.

In *d'Onofrio et al.*, the total amount of applied drugs is limited. To be able to treat this constraint in our optimization framework, we add two auxiliary states which sum up the amounts of given drugs:

$$\dot{x}_2(t) = u_0(t), \tag{6}$$
$$\dot{x}_3(t) = u_1(t). \tag{7}$$

Thus, the complete model is described by the system

$$\dot{x}_0(t) = -\zeta\, x_0(t) \ln\left(\frac{x_0(t)}{x_1(t)}\right) - F\, x_0(t)\, u_1(t), \tag{8a}$$
$$\begin{aligned}\dot{x}_1(t) = {} & b\, x_0(t) - \mu\, x_1(t) - d\, x_0(t)^{\frac{2}{3}} x_1(t) \\ & - G\, u_0(t)\, x_1(t) - \eta\, x_1(t)\, u_1(t),\end{aligned} \tag{8b}$$
$$\dot{x}_2(t) = u_0(t), \tag{8c}$$
$$\dot{x}_3(t) = u_1(t). \tag{8d}$$

for $t \in [t_0, t_f]$.

The parameters G, b, d, μ, ζ, γ in [5] have been derived by about 1,000,000 runs of a Monte-Carlo algorithm based on data from experiments with mice that have been injected Lewis lung carcinoma cells. Note that the parameters and bounds F, η, A, a, C, c (compare also Section 3) are neither taken from [5] nor based on experimental data. These values have been used for numerical experiments only.

2.2. De Pillis et al. (2006)

The model by *de Pillis et al. (2006)* [3] consists of six states, three controls and 29 parameters in three parameter sets. The work is based on previous work by the same or some of the authors [8, 15, 16].

As a major difference to the model above, it contains a combination of *chemotherapy* and *immunotherapy*. The first state is again the tumor population x_0, but now measured in absolute cell count. Instead of the blood vessel volume, this model features three types of immune cell populations, all measured in absolute cell count. NK cells x_1 – unspecific immune cells which are also present in a healthy body ("natural killer" cells) – , $CD8^+$ T cells x_2 – tumor-specific cytotoxic T-cells –, and circulating lymphocyte pool x_3.

The fifth and the sixth state represent the chemotherapeutic drug concentration x_4 respectively *Interleukin-2 (IL-2)* concentration x_5. *IL-2*, which is one of the two *immunotherapeutic* controls, is a cytokine that stimulates $CD8^+$ T activation cells and is used "to boost immune system function" [3]. In addition, there is a control for a classic *cytostatic drug* u_0 and one for a *tumor infiltrating lymphocyte* injection (*TIL*) u_2. The latter means an injection of $CD8^+$ T cells that have been stimulated against tumor cells outside the body.

The model is described by the following system of ODEs. In favor of readability we omit the time dependence of states and controls. For more details on the equations we refer to [3] and [15].

$$\begin{aligned}\dot{x}_0 &= a\,x_0\,(1 - b\,x_0) - c\,x_1\,x_0 - D\,x_0 \\ &\quad - K_T\,(1 - \mathrm{e}^{-x_4})\,x_0,\end{aligned} \tag{9a}$$

$$\begin{aligned}\dot{x}_1 &= e\,x_3 - f\,x_1 + g\,\frac{{x_0}^2}{h + {x_0}^2}x_1 - p\,x_1\,x_0 \\ &\quad - K_N\,(1 - \mathrm{e}^{-x_4})\,x_1,\end{aligned} \tag{9b}$$

$$\begin{aligned}\dot{x}_2 &= -m\,x_2 + j\,\frac{D^2\,{x_0}^2}{k + D^2\,{x_0}^2}x_2 - q\,x_2\,x_0 \\ &\quad + (r_1\,x_1 + r_2\,x_3)\,x_0 - v\,x_1\,{x_2}^2 \\ &\quad - K_L\,(1 - \mathrm{e}^{-x_4})\,x_2 + \frac{p_I\,x_2\,x_5}{g_I + x_5} + u_2,\end{aligned} \tag{9c}$$

$$\dot{x}_3 = \alpha - \beta\,x_3 - K_C\,(1 - \mathrm{e}^{-x_4})\,x_3, \tag{9d}$$

$$\dot{x}_4 = -\gamma\,x_4 + u_0, \tag{9e}$$

$$\dot{x}_5 = -\mu_I\,x_5 + u_1 \tag{9f}$$

for $t \in [t_0, t_\mathrm{f}]$ and the shortcut $D = d\,\frac{(x_2/x_0)^l}{s + (x_2/x_0)^l}$.

Three parameter sets can be found in the literature: *mouse*, *human 9*, and *human 10*. As the name suggests, the *mouse* parameter set contains numerical values derived from murine experimental data. In fact, the parameters come from different papers treating different types of cancer and different types of mice. For example the *tumor growth parameter a* has been fitted to data from a paper by *Diefenbach et al.* [17]. In that article, *EL4* thymoma, *RMA* lymphoma and *B16-BL6* melanoma have been implanted into *B6-Rag*$^{-/-}$ mice. On the other hand, e.g., the death rate of NK cells f is derived from *Kuznetsov et al.* [18], where a mathematical model is used to describe the kinetics of growth and regression of a BCL_1 lymphoma in *BALB/c* mice. For the parameters r_2 and v, no source is provided.

For the *human* parameter sets, the authors refer to an article by *Dudley et al.*[4]. This publication contains real proband data of 13 melanoma patients. The data of the ones numbered 9 and 10 have been used in [3] for fitting seven of the parameters. Again, for r_2 and v, no source is provided. Actually, there are eight more references for the *human* parameter set, e.g., the two murine papers from the *mouse* parameter set. Another source [19] refers among others to *Kuznetsov et al.* Note that this means that about one third of the *human* parameters comes from *murine* experiments.

In [19] it is stated that the value of a certain parameter in their model "(...) varies greatly from patient to patient and cancer to cancer." So this model may generally not be adequate for generating useful treatment schedules – in particular for humans since there is only little human data used and the values may highly depend on the patient and the type of cancer. But it still may be useful for making general qualitative statements.

In summary, the heterogeneity of model parameters makes an applicability of numerical results obtained by us or other authors in clinical practice improbable.

2.3. Other Approaches

Finally we give a short survey on models we did not consider in detail. There are lots of different mathematical modeling approaches in the cancer chemotherapy context, so we restrict ourselves to some that are conceptually close to the ones presented above.

2.3.1. Ergun et al.

The model in *Ergun et al.* [6] is – similar to the one presented in section 2.1 – a modification of the *Hahnfeldt*-model [5]. In this article, a combination of radiotherapy and anti-angiogenic therapy is investigated. The major difference in the model is the decoupling of the vasculature equation from tumor volume by simply replacing tumor volume by vasculature volume. For the radiotherapy an *LQ* model is used. The authors report on several optimal control results. There is also a detailed analysis of the combination therapy for a slightly modified version of the model by *Ledzewicz et al.* [20]

2.3.2. Chareyron and Alamir

The work by *Chareyron and Alamir* [10] is based on the work by *de Pillis et al.* [8, 15, 16, 3]. The authors use

the model presented in section 2.2 to apply *nonlinear model predictive control* (*NMPC*) techniques.

However, only the chemotherapy control is considered for the NMPC scheme while both the immunotherapy and the TIL are derived by *indirect methods* independently from the chemotherapy. The chemotherapy itself is fixed to a finite set of values (0%, 20%, 40%, 60%, 80%, and 100% of maximum). This means that effectively chemotherapy is not a continuous control but a mixed-integer one. Since NMPC techniques are not part of our work and we also want to study optimal control of *continuous* chemotherapy here, we did not further pursue the approach of *Chareyron and Alamir*.

2.3.3. De Pillis et al. (2001)

The model of *De Pillis et al. (2001)* [8] is one of the "ancestors" of *de Pillis et al. (2006)*. It only includes a cytostatic chemotherapy control. An optimal control problem is formulated (minimize tumor size at end time subject to the number of "normal" cells is above some lower bound) and optimal control results are presented. With one control and the constraint on normal cells, surprising results are not to be expected and indeed the optimal schedules show a bang-bang-structure.

We wanted to verify these results in our optimization framework, but some of the model's parameters are only given in relations or intervals (e.g., "$0 \leq s \leq 0.5$", "$a_3 \leq a_1 \leq a_2$"). Since it was not possible to get the exact parameter values from the authors, this approach was not subject of further investigations.

2.3.4. De Pillis et al. (2008)

In analogy to *de Pillis et al. (2006)* [3] essentially derived from previous work by the authors, *de Pillis et al. (2008)* [9] can be considered a descendant model of *de Pillis et al. (2006)*. It contains the same controls and states as the one discussed in Section 2.2.

In contrast to its predecessor, the latter article focuses on optimal control results. There are some modifications of the equations, but overall they are very similar. Most of the parameters have been adapted either from the *mouse* or the *human 9*/*human 10* sets. At least some of the changes in the model equations compared to [3] may be due to the tractability with an *indirect optimal control approach*. As an example, the saturation term for the influence of chemotherapy ($1 - \mathrm{e}^{-x_4(t)}$) has been replaced by the drug concentration x_4, significantly facilitating the analytical work of the *first optimize, then discretize* approach chosen by the authors.

We could not reproduce the numerical results on the basis of the equations and the parameter set given in the article. However, with a modified tumor growth parameter (4.0 instead of $2.0 \cdot 10^{-3}$) we succeeded to reproduce some optimal controls result of a first scenario. For a second scenario, we could mostly reproduce the result choosing again a different tumor growth parameter (2.0). Our attempts to contact the authors to resolve these deviations have not been successful. As it is not clear where the differences originate from, especially as they do not seem to derive from a single wrong parameter value, we eventually decided to not further investigate this model. Details on our simulation and optimization studies can be found in [21].

2.3.5. Isaeva and Osipov

The article by *Isaeva and Osipov* [11] is similar to *de Pillis et al. (2006)* as it also takes classical chemotherapy and two types of immunotherapy into account, but the model also shows some differences. For example, they use *Gompertz growth* instead of *logistic growth* and just one state for immune cell populations. Because of the structural similarities to *de Pillis et al. (2006)*, we decided to investigate only one of the two similar approaches.

3. Chemotherapy Control Problems

Our goal is to investigate properties of optimal solutions based on the ODE models in Section 2. This includes the definition of an objective function, initial values, as well as constraints the trajectories have to fulfill.

D'Onofrio et al. formulated an optimal control problem for the model. The objective function supposed to be minimized is

$$x_0(t_\mathrm{f}) \; + \; \alpha \int_{t_0}^{t_\mathrm{f}} u_0(t)^2 \quad \mathrm{d}t, \tag{10}$$

while the end time t_f is free and α is small. Apparently a value of $\alpha = 0.005$ has been used in [7] to identify the correct control switching structure, whereas a value $\alpha = 0$ has been used for the final calculation of the objective value. In [3] no control problem was specified, whereas in [9] a weighted sum was used. In our study we use the weighted sum

$$p_0 \cdot x_0(t_\mathrm{f}) + \int_{t_0}^{t_\mathrm{f}} p_1 \cdot x_0(t)^2 \; \mathrm{d}t + \sum_{i=0}^{n_u - 1} \int_{t_0}^{t_\mathrm{f}} p_{i+2} \cdot u_i(t) \; \mathrm{d}t \tag{11}$$

with a L^1 penalization of the positive controls. For $\alpha = 0$ the objective (10) is a special case of (11). We will

Name	$x_0(t_0)$	$x_1(t_0)$	$x_2(t_0)$	$x_3(t_0)$	$x_4(t_0)$	$x_5(t_0)$	Parameter set
(T1)	$1 \cdot 10^6$	$5 \cdot 10^4$	$1 \cdot 10^2$	$1.1 \cdot 10^7$	0	0	Mouse
(T2)	$1 \cdot 10^6$	$1 \cdot 10^5$	$1 \cdot 10^2$	$6 \cdot 10^{10}$	0	0	Human 9/10
(T3)	$1 \cdot 10^6$	$1 \cdot 10^3$	1	$6 \cdot 10^8$	0	0	Human 9
(T4)	$2 \cdot 10^7$	$1 \cdot 10^3$	1	$6 \cdot 10^8$	0	0	Human 9
(T5)	$1 \cdot 10^8$	$1 \cdot 10^3$	1	$6 \cdot 10^8$	0	0	Human 9/10
(T6)	$1 \cdot 10^7$	$1 \cdot 10^3$	1	$6 \cdot 10^8$	0	0	Human 9
(T7)	$1 \cdot 10^5$	$1 \cdot 10^5$	$1 \cdot 10^2$	$6 \cdot 10^{10}$	0	0	Human 10

Table 1: Initial values used for *de Pillis et al. (2006)*. "Parameter set" indicates for which of the three parameter sets "mouse", "human 9", and "human 10" the initial values have been used in this article.

compare the influence of different objective functions in Section 5, in particular,

$$\begin{aligned}
&p_0 = 1, && p_1 = 0, && p_2 = 0, && \text{(O1)}\\
&p_0 = -1, && p_1 = 0, && p_2 = 0, && \text{(O2)}\\
&p_0 = 5 \cdot 10^{-3}, && p_1 = 10^{-11}, && p_2 = 10^4, && \text{(O3)}\\
&p_0 = -5 \cdot 10^{-3}, && p_1 = -10^{-11}, && p_2 = 10^4, && \text{(O4)}\\
&p_0 = 1, && p_1 = 0, && p_2 = 1, && \text{(O5)}\\
&p_0 = -1, && p_1 = 0, && p_2 = 1, && \text{(O6)}\\
&p_0 = 1, && p_1 = 10^{-6}, && p_2 = 10^{-2}, && \text{(O7)}
\end{aligned}$$

with $p_3 = p_4 = 0$ in all cases. We will later identify these parameter sets with an objective function, e.g., refer in short to (O1) as the objective function (11) with values for p_0, p_1, p_2 defined by (O1).

The trajectories are constrained in the following way. For all control problems we have the inequalities

$$0 \le u_i(t) \le u_i^{\max}, \qquad 0 \le x_i(t). \tag{12}$$

For the control problems based on the model of *d'Onofrio et al.* we furthermore consider a maximal dose over the whole time horizon in the form

$$x_2(t) \le x_2^{\max}, \qquad x_3(t) \le x_3^{\max} \tag{13}$$

We will consider different scenarios in Section 5. In our context a scenario consists of a set of initial values and values for the upper bounds in (12) and (13). For the control problems solved in Section 5.1 we fix $x_2(0) = x_3(0) = 0$ and $u_0^{\max} = 75, x_2^{\max} = 300$ in all cases and define

$$\begin{aligned}
&x_0(0) = 12000, && x_1(0) = 15000, && \text{(S1)}\\
&u_1^{\max} = 1, && x_3^{\max} = 2.\\
&x_0(0) = 12000, && x_1(0) = 15000, && \text{(S2)}\\
&u_1^{\max} = 2, && x_3^{\max} = 10.\\
&x_0(0) = 14000, && x_1(0) = 5000, && \text{(S3)}\\
&u_1^{\max} = 1, && x_3^{\max} = 2.\\
&x_0(0) = 14000, && x_1(0) = 5000, && \text{(S4)}\\
&u_1^{\max} = 2, && x_3^{\max} = 10.
\end{aligned}$$

For the solutions of the control problems presented in Sections 5.2 to 5.4 the upper bounds are given by $u_0^{\max} = 1$, $u_1^{\max} = 5 \cdot 10^6$, and $u_2^{\max} = 0$. Note that for the *tumor infiltrating lymphocytes (TIL)* control $u_2(\cdot)$ no bounds were given in the original paper, therefore we fixed $u_2(\cdot)$ to zero for this study. The value of the fixed end time t_f varies in our scenarios and can be seen in the plots. The resulting scenarios are defined by different initial values listed in Table 1.

4. Direct Multiple Shooting

We give a short introduction to *Bock's direct multiple shooting method*, developed by *Georg Bock* and coworkers [22] in the early 1980s. More information on this technique can be found, e.g., in [23].

4.1. Problem Formulation

The following *optimal control problem* represents the class of problems we want to solve in this article:

$$\min_{x,u,p} E(x(t_f)) + \int_{t_0}^{t_f} L(t, x(t), u(t), p)\, \mathrm{d}t \tag{14a}$$

$$\text{subject to} \quad \dot{x}(t) = f(t, x(t), u(t), p), \tag{14b}$$
$$x(t_0) = x_s, \tag{14c}$$
$$0 = r_e(x(t_0), x(t_f), p), \tag{14d}$$
$$0 \le r_i(x(t_0), x(t_f), p), \tag{14e}$$
$$0 \le g(t, x(t), u(t), p), \tag{14f}$$

for $t \in [t_0, t_f]$ almost everywhere, with *differential states* $x : [t_0, t_f] \to \mathbb{R}^{n_x}$, *control functions* $u : [t_0, t_f] \to \mathbb{R}^{n_u}$, fixed *model parameters* $p \in \mathbb{R}^{n_p}$, and an *objective function* of *Bolza type*, all functions assumed sufficiently smooth.

Let x and u be the vectors of states x_i and controls u_i, then equation (14b) represents the ODE model with a right hand side f depending on *time* $t \in [t_0, t_f]$ and initial values x_s are given in (14c). In (14d) and (14e) equality respectively inequality boundary conditions are summarized, and (14f) contains state and path constraints.

4.2. Discretization of States and Controls

In the articles mentioned in section 2, mostly *indirect methods* have been used, when optimal control was considered. These methods build on the necessary conditions of optimality in function space, *Pontryagin's maximum principle*, and apply an appropriate discretization to solve the resulting boundary value problem.

In contrast, our *first discretize, then optimize* approach transforms the control problem first to a nonlinear program (NLP), before this finite-dimensional optimization problem is solved to optimality. We start with the discretization of the controls. The continuous controls are replaced by *base functions* with local support, such as piecewise constant or piecewise linear functions. These functions can be described by finitely many parameters. To do so, we select a time grid

$$t_0 = \tau_0 < \tau_1 < \cdots < \tau_m = t_f, \quad m \in \mathbb{N} \tag{15}$$

and with $I_i := [\tau_i, \tau_{i+1}]\ \forall\, i \in \{0, \ldots, m-1\}$ set

$$u(t)\Big|_{I_i} = \phi_i(t, w_i), \quad w_i \in \mathbb{R}^{\mu_i}, \tag{16}$$

where the ϕ_i are the base functions. Now we have transformed the infinite-dimensional control u into a finite vector $w = (w_0, \ldots, w_{m-1})$. For notational convenience we omit the parameter vector p in the following.

The states x are discretized using *multiple shooting*. We have to choose a time grid again and for efficiency and simplicity we choose the same grid as for the controls. In theory, this is no limitation of generality, as we could refine the grids such that they match and add some constraints. We introduce $m+1$ new variables $s_0, \ldots, s_m$ which represent the initial values of the ODE on each interval I_i respectively the final value s_m. Now we solve m independent *initial value problems* $\forall\, i \in \{0, \ldots, m-1\}$,

$$\dot{x}(t; \tau_i, s_i) = f(t, x_i(t), \phi_i(t, w_i)), \tag{17a}$$
$$x(\tau_i; \tau_i, s_i) = s_i, \tag{17b}$$
$$t \in [\tau_i, \tau_{i+1}]. \tag{17c}$$

For the numerical results presented in this paper, a BDF-based DAE solver, *DAESOL* [30], has been used to solve the initial value problems. Note that the method is exact if the initial value problems are solved exactly.

To ensure equivalence to the original problem, we have to add *matching conditions*, which are the equality constraints

$$s_{i+1} = x(\tau_{i+1}; \tau_i, s_i) \quad \forall\, i \in \{0, \ldots, m-1\}. \tag{18}$$

The objective function is separable, so it can be computed separately on each interval by

$$\int_{t_0}^{t_f} L(t, x(t), \phi(t, w))\, \mathrm{d}t = \sum_{i=0}^{m-1} L_i(\tau_{i+1}) \tag{19}$$

$$\text{with } L_i(t) = \int_{\tau_i}^{t} L(t', x(t'; \tau_i, s_i), \phi_i(t', w_i))\mathrm{d}t' \tag{20}$$
$$\text{and } \phi(t, w) := \phi_i(t, w_i) \text{ for } t \in I_i. \tag{21}$$

The continuous constraints $g(t, x(t), u(t), p) \ge 0$ are evaluated pointwise on the grid (for ease of notation, we write $x(\tau_m; \tau_m, s_m) := x(\tau_m; \tau_{m-1}, s_{m-1})$ and $\phi_m(\tau_m, w_m) := \phi_{m-1}(\tau_m, w_{m-1})$ from now on):

$$g(\tau_i, x(\tau_i; \tau_i, s_i), \phi_i(\tau_i, w_i)) \ge 0, \ \forall\, i \in \{0, \ldots, m\}. \tag{22}$$

Finally, transformed boundary conditions and initial values read

$$r(s_0, s_m) = 0, \tag{23a}$$
$$s_0 = x_s. \tag{23b}$$

4.3. Solution of the NLP

We have transformed the infinite-dimensional optimal control problem (14) into a finite-dimensional NLP.

By defining $y := (s_0, w_0, \ldots, s_{m-1}, w_{m-1}, s_m)$, we obtain

$$\min_{y} \quad E(s_m) + \sum_{i=0}^{m-1} L_i(\tau_{i+1}) \tag{24a}$$

$$\text{s.t.} \quad 0 = s_{i+1} - x(\tau_{i+1}; \tau_i, s_i) \; \forall\, i \in \{0, \ldots, m-1\}, \tag{24b}$$

$$0 \le g(\tau_i, x(\tau_i; \tau_i, s_i), \phi_i(\tau_i, w_i)) \; \forall\, i \in \{0, \ldots, m\}, \tag{24c}$$

$$0 = r_e(s_0, s_m), \tag{24d}$$

$$0 \le r_i(s_0, s_m), \tag{24e}$$

$$0 = s_0 - x_s. \tag{24f}$$

This NLP is solved with a sequential quadratic programming (SQP) method. This technique has been introduced by *Wilson* [31], *Han*, and *Powell* [32].

The NLP (24) can be written in the form

$$\min_{x} \quad f(x) \tag{25a}$$

$$\text{subject to} \quad g(x) = 0, \tag{25b}$$

$$h(x) \ge 0, \tag{25c}$$

with generally nonlinear f, g, and h. Instead of considering this problem, starting with some initial value x^0, we compute the iterates x^k with a step size $t^k \in (0, 1]$,

$$x^{k+1} = x^k + t^k \Delta x^k, \tag{26}$$

by solving a related quadratic program (QP),

$$\min_{\Delta x} \quad \frac{1}{2} \Delta x^T H^k \Delta x + \nabla f(x^k)^T \Delta x \tag{27a}$$

$$\text{subject to} \quad g(x^k) + \nabla g(x^k)^T \Delta x = 0, \tag{27b}$$

$$h(x^k) + \nabla h(x^k)^T \Delta x \ge 0, \tag{27c}$$

where H^k is set, e.g., to the Hessian of the Lagrangian of the problem or some approximation of this Hessian. We compute the step size by a *line search*.

This is equivalent to a Newton-type method. For more information we refer to relevant literature, e.g., to *Nocedal and Wright* [33].

The Hessian resulting from the multiple shooting discretization features a special structure which can and needs to be exploited in the SQP algorithm, [23].

5. Numerical Results

In this section, we present numerical results for the control problems that have been introduced in Sections 2 and 3 obtained by applying Bock's direct multiple shooting algorithm from Section 4. This section is split into a subsection for each model and parameter set we investigated.

5.1. d'Onofrio et al.

We tried to reproduce the results from the paper [7] first. Optimal solutions for each scenario are depicted in Figures 1 left and 3. One can conclude from the plots that the results could be essentially reproduced on the whole, especially the control structure is the same. However, the end times in our results differ to some extent (0.13% or less) from those in *d'Onofrio et al.* – e.g., 6.653 vs. 6.648 (0.08%) in scenario (S1). The differences between the tumor volumes are much smaller (in each case less than 0.01%), between vasculature volumes a little higher (1.47% or less): 7019.29 vs. 7019.09 for tumors and 7294.18 vs. 7365.33 for vasculature in scenario (S1) for example, which corresponds to 0.003% respectively 0.97%. The differences in the other scenarios are in a similar range and might be due to differences in the discretization. All solutions have been computed with 100 multiple shooting nodes in our case.

A reasonable question one may ask is how much can be gained by optimal control of chemotherapy treatment schedules. For this purpose, we changed the objective function to (O2), $\min -x_0(t_f)$, and computed an optimal control for (S1) with end time fixed to $t_f = 6.653$ and the amount of drugs given over the total time fixed to the bounds 300 respectively 2. This corresponds to a maximization of the tumor size at the end time. The result is shown in Figure 1 together with a simulation without any therapy. Tumor volume under maximization is at 7979.50, which is about 40.5% lower than the volume without any treatment (13419.80) on the one hand, but on the other hand 13.7% higher than the volume under the optimal control (7019.29).

One observes a different structure of the optimal control, which is almost of bang-bang type for both control functions. Obviously, under a maximization of the tumor volume it is optimal (in this model) to administer a large amount of the drugs at the beginning of treatment, because the fraction of cells killed is lower when the tumor and vessel volumes are relatively small. As angiogenic treatment has a delayed influence on the tumor volume, the full-dose part at the end of the time scale does not play a role for the development of tumor volume.

In summary, we compared solutions for minimal and maximal tumor value for the first time in this model. The optimal chemotherapy controls that have been plotted in Figure 1 can be intuitively understood on the basis of the model, as they are related to the Gompertz-type growth of the tumor. However, the observed difference of about 10% is, in particular when considering the high

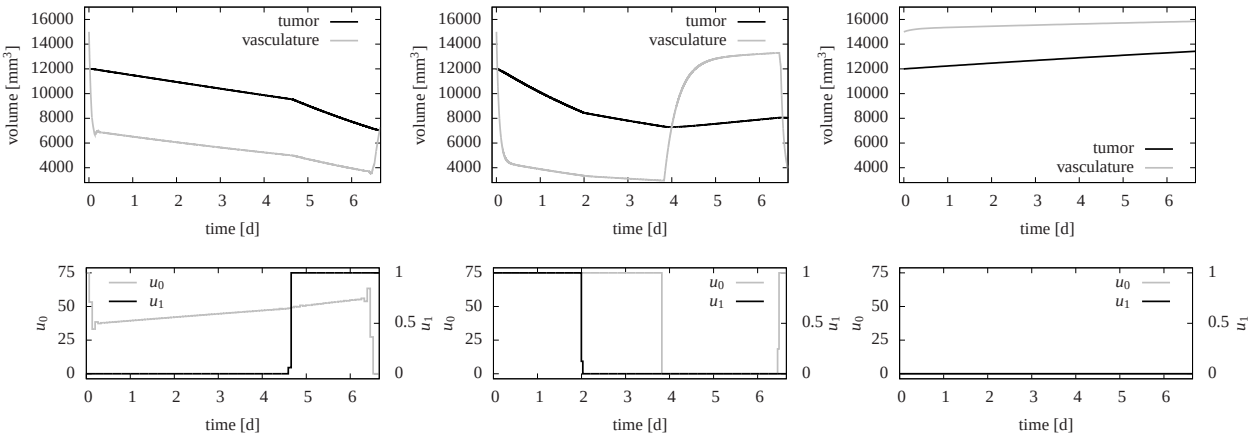

Figure 1: Optimization results for *d'Onofrio et al.*. Upper row: tumor (dark) and vasculature (bright) volume. Lower row: anti-angiogenic (bright, u_0) and chemotherapy (dark, u_1) controls. All results for scenario (S1) for different objective functions. Left: minimization of tumor volume at end time, objective (O1). Middle: maximization of tumor volume at end time, (O2). Right: no therapy (controls both at lower bound). The end value of the tumor population under maximization (with the same t_f) is about 10% higher than the minimized value, which is the maximal difference due to bad timing of drug admission.

uncertainty of model and parameters, not highly encouraging for practical improvements. This conclusion is supported by the results for different objective functions which show that the reduction in tumor size is strongly dependent on the amount of drugs, not so much on the timing of its application.

5.2. "mouse", de Pillis et al. (2006)

In this section, we present optimal control results for the *mouse* parameter set, which is one of three parameter sets in *de Pillis et al. (2006)* [3].

For all three parameter sets we consider a fixed time horizon of either $t_f = 40$ or $t_f = 120$ days, as in [3]. In [21] also scenarios with free end time can be found. As stated before, we did not consider *tumor infiltrating lymphocytes (TIL)*, as more modeling work is necessary to come up with realistic bounds here. For the mouse model which contains no *IL-2* therapy, this means we consider a classical cytostatic chemo-monotherapy. As in *De Pillis et al.* we choose $u_0^{\max} = 1$ for numerical experiments.

There are seven different initial value sets in [3], see Table 1. Note that only ($T1$) has been used for the "mouse" model.

For the verification of the models' implementations in our optimization framework we ran several simulations. The results of [3] for the *mouse* set could be reproduced, for chemotherapy as well as without any therapy, [21]. Optimal control results of the *mouse* model are shown in Figures 5 and 6.

For $t_f = 40$ and the weighted sum objective (O3) we fixed the total amount of drugs applied to the values of the optimal solution, changed the sign of p_0 and p_1. This corresponds to a maximization of the tumor over the whole time horizon and at the end time in the given relative weighting under the constraint of a given total amount of drugs. We also compare the minimization result to a "standard treatment" as applied by *de Pillis et al.* in Figure 5. The potential benefit of optimal control is much higher in this scenario compared to the results in Section 5.1. While the maximized tumor at the end time is at about $2 \cdot 10^7$ cells, the minimal value is only about 10^5 cells. This corresponds to 0.5% of the maximal value. The tumor size for the standard treatment is even higher than the maximized one, but again the total amount of drugs given is significantly lower here.

Considering the high potential for correct timing of drug administration in this case, the question which objective function should be used becomes more important. In Figure 6 left and right one observes that under the weighted sum objective (O3) tumor cells are on a lower level in general whereas the end level is orders of magnitude lower with (O5) (middle plot).

Figure 6 right shows an alternative local minimum to Figure 6 left. While one solution applies chemotherapy early, hence reducing the tumor volume to a low value in the first half of the time horizon and letting it grow in the second half, the solution on the left allows for a higher value in the first part to reduce it in the second. Both strategies are related to the Gompertz growth of the tumor — if the tumor volume is high, the growth rate

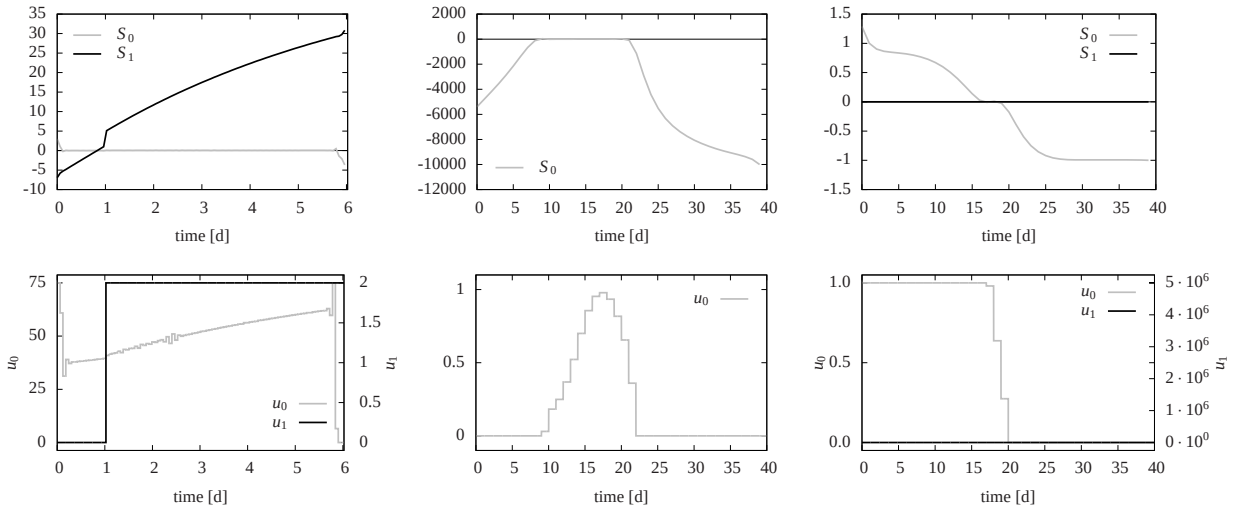

Figure 2: Switching functions ...

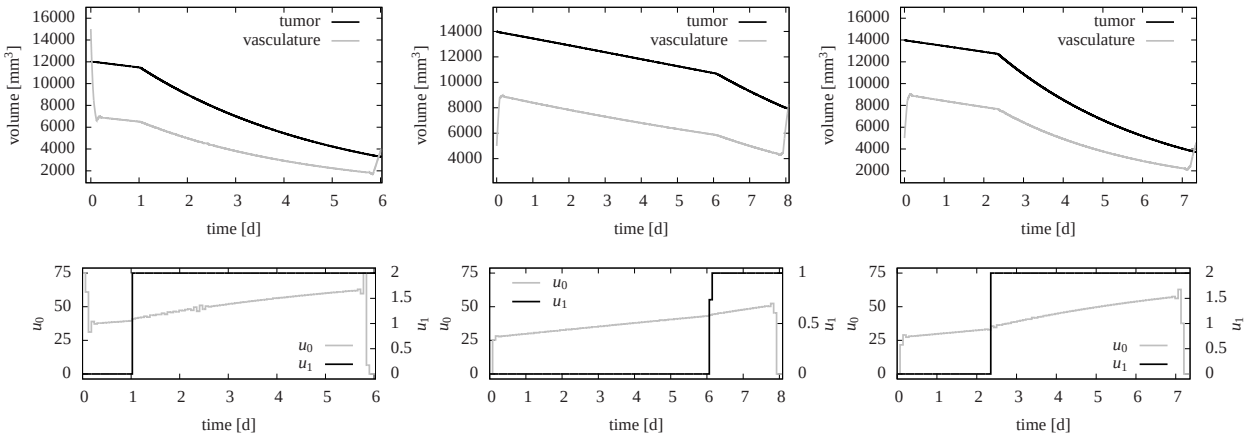

Figure 3: Trajectories as in Figure 1. Optimization results for *d'Onofrio et al.*, scenarios (S2), (S3), (S4) from left to right, all with objective (O1), minimization of tumor at end time. All solutions are structurally similar.

is considerably lower. Therefore a strategy distributing the chemotherapy over time would lead to a (nonoptimal) higher average growth rate.

5.3. "human 9", de Pillis et al. (2006)

The *human 9* model is the second parameter set from *de Pillis et al. (2006)*. We picked out two scenarios to verify our implementation, see [21]. The maximal dose of chemotherapy has been changed to 5.0, but there is no reason given for the higher dose. The immunotherapeutic pulses are said to be at $5.0 \cdot 10^6$ in one experiment and at $5.0 \cdot 10^5$ in another one. Maybe the latter is a typing error, as the upper bound of both *IL-2* concentration plots is $5.0 \cdot 10^5$, which makes sense for a dosage of $5.0 \cdot 10^6$ with the corresponding equation (9f). Eventually we decided to adopt 1.0 respectively $5.0 \cdot 10^6$ as upper bounds for the chemotherapeutic respectively immunotherapeutic control. For chemotherapy, the drug amount applied in our solutions is notably higher than in the *standard* treatments investigated in [3], so it might be reasonable to consider a smaller upper bound. Additionally, note that the *human* parameter sets are based on mostly *murine* data. Some remarks on the immunotherapy level will follow below.

First, we have a look at the comparison between maximized and minimized tumor populations, see Figure 7. The procedure was the same as in the *mouse* Section. We fixed the drug amount to the minimization value and

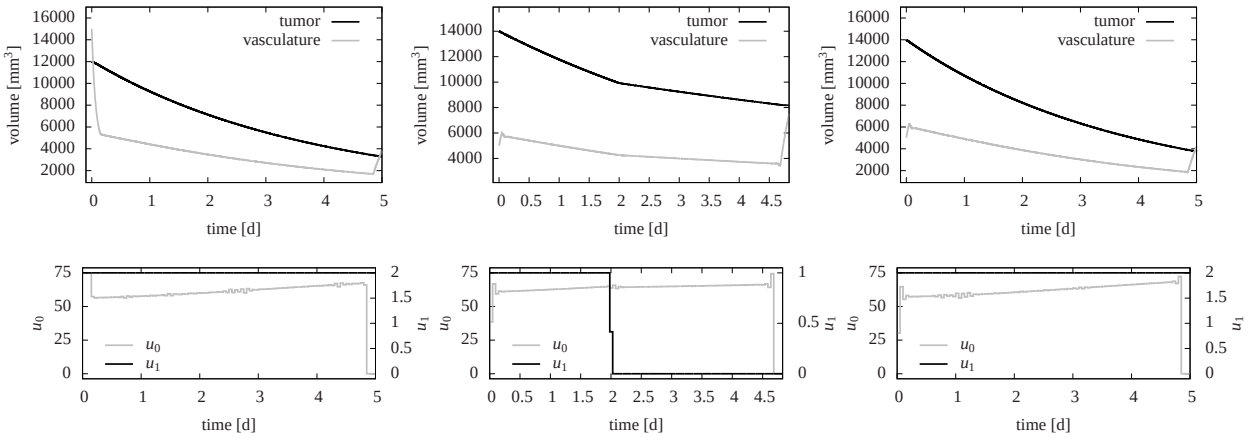

Figure 4: Trajectories as in Figure 3, now with objective (O7) which includes impact of the L^2 norm. Although $x_0(t_f)$ is of comparable size, controls, end time t_f, and trajectories differ considerably compared to the objective in Figure 3.

changed the sign of the corresponding objective parameters, i.e., $p_0 = -1.0$ for the objective with a penalty on u_0. The difference is even higher here with a maximal tumor of almost 10^9 and a minimum one with less than 1, which is less than 0.000001‰. Again the standard treatment is worse than the maximization, however, the drug amount for the maximization was about 250% of the standard treatment.

Figure 8 contains representative optimization results for different initial values and objective functions. While Figure 8 center features a full dose chemotherapy, in Figures 8 left there is a full dose part at the beginning followed by a short singular arc leading into a zero part. A similar solution occurs in some more scenarios of *human 9* (data not shown) and a free end time scenario ($t_f \approx 26$) looks very similar, too. Figure 8 right shows the problem of a delayed therapy – if the objective is to minimize tumor volume at the end time and the time horizon is large, the result may be long time periods (65 days Figure 8 right) with a high tumor volume before therapy starts.

Except for one scenario, immunotherapy does not play a significant role in the treatment. Often it is at such a low levels (e.g., 10^{-7} with an upper bound of $5 \cdot 10^6$) that it might not be be considered therapeutic at all. Note also that none of the objective functions contains a penalty on the immunotherapeutic control u_1, so immunotherapy might dissappear completely with a penalty. However, there are also mathematical reasons for this low influence of immunotherapy. The control u_1 enters only in equation (9f), which reads

$$\dot{x}_5 = -\mu_I \, x_5 + u_1. \tag{28}$$

With a full dose of $u_1(t) = 5.0 \cdot 10^6$ and $\mu_I = 10$, $x_5(t)$ should be at about $5.0 \cdot 10^5$ close to a steady state. The state x_5 itself only plays a role in equation (9c), where the corresponding terms are

$$\dot{x}_2 = \cdots + \frac{p_I \, x_2 \, x_5}{g_I + x_5} + \ldots \tag{29}$$

with $p_I = 1.25 \cdot 10^{-1}$ and $g_I = 2 \cdot 10^7$. For a x_2 which is most of the time at a level of at least 10^5, we have

$$\frac{p_I \, x_2 \, x_5}{g_I + x_5} \approx \frac{10^{-1} \, 10^5 \, 10^5}{10^7 + 10^5} \approx \frac{10^9}{10^7} \approx 10^2 \tag{30}$$

and the influence of a 10^2 term on a 10^5 state indeed should be low. We conclude that additional work on the modeling of immunotherapy influences is necessary.

5.4. *"human 10", de Pillis et al. (2006)*

Like *human 9*, the *human 10* parameter set shares the equations with the *mouse* model. Considering reproduction of the results in the *de Pillis et al.* article, the first two scenarios without any treatment could be verified. In other scenarios, we observed some differences or they could not be reproduced at all. The differences seem to arise from the influence of *IL-2*, compare [21] for a detailed discussion.

In Figures 9, 10, and 11 we show optimal controls for different initial values from Table 1, end times t_f, and objective functions.

We again compare maximization and minimization and a *standard* treatment in Figure 9.

A selection of optimal solutions is presented in Figures 10 and 11. Immunotherapy is again on a very low

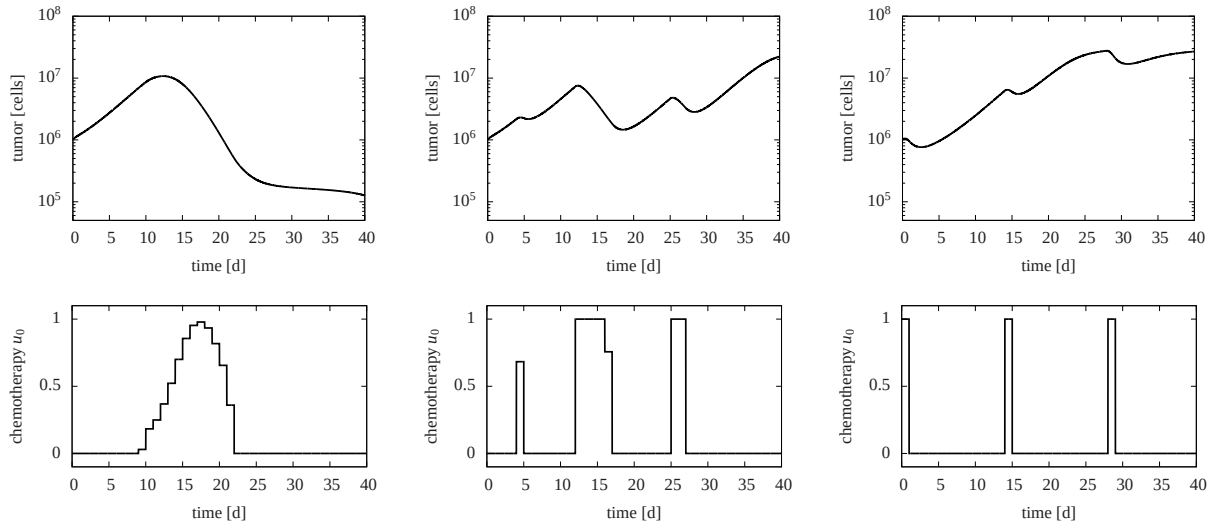

Figure 5: Optimization results for *de Pillis et al. (2006), mouse*, scenario (T1). Upper row: tumor population. Lower row: chemotherapy control u_0. Left: minimization of weighted objective (O3). Middle: maximization of weighted objective (O4). Right: standard therapy (example from [3]). The end value of the tumor population under minimization is about two orders of magnitude below the maximized (worst) one. Note that the given drug amount in the standard treatment is significantly lower, so that the result is even worse than for maximization.

levels as expected. Many solutions for chemotherapy show a singular arc (Figure 10 center and Figure 11 throughout). Note that these solutions have been computed for the weighted sum objective. Only 11 right contains a singular solution with minimization of the tumor at the and time with a penalty on chemotherapy. Further results, including free end time scenarios and the calculation of *sparse controls*, can be found in [21].

6. Conclusion and Outlook

We presented optimal control results for four different cancer chemotherapy models based on two sets of ordinary differential equations. Not all of the previous simulation results in the literature could be verified, e.g., *de Pillis et al. 2008*, [9], see [21] for a detailed discussion. As the general purpose software package MUSCOD-II has been successfully applied to hundreds of different applications, and we cross-checked our problem-dependent implementation of the equations, we suspect inconsistencies in the published model, in particular in some parameter values.

Our optimal control solutions of the *d'Onofrio* model nearly quantitatively match the ones in their article [7]. But we also study additional optimization scenarios. The three different models based on *de Pillis et al. (2006)* have been solved to optimality for the first time to the best of our knowledge.

In order to estimate the potential for the correct timing of chemotherapies we proposed to compare the results of a minimization to the ones of a maximization with the same total amount of drugs. The ratio between these two values is an indicator for the potential gain. For the d'Onofrio model in Section 5.1 this potential is rather low. A comparison to a maximization of the tumor at the end time with fixed drug amounts showed that tumor size is only about 15% larger in the worst treatment scenario, which can nevertheless be clinically significant. The optimal treatment yields a tumor 40% smaller than in the case without any treatment.

For the control problems based on the *de Pillis* model, Sections 5.2, 5.3, and 5.4, the difference between minimimal and maximal objective is several orders of magnitude, indicating a high potential for optimal timing.

In this context the question of how to define the objective function naturally becomes more important. We considered different terms in a weighted sum objective function: tumor population at the end time and integrated over the whole time horizon, as well as possible penalizations of the controls. A high dependency of the results on the weights could be shown. For certain scenarios a control strategy leads to a complete removal of the tumor at the end time at the price of a higher average value, whereas an optimal control taking the L^2 norm into account generally does not lead to a removal. From the point of view of potential clinical applications, a tradeoff between minimal end size of the tumor and

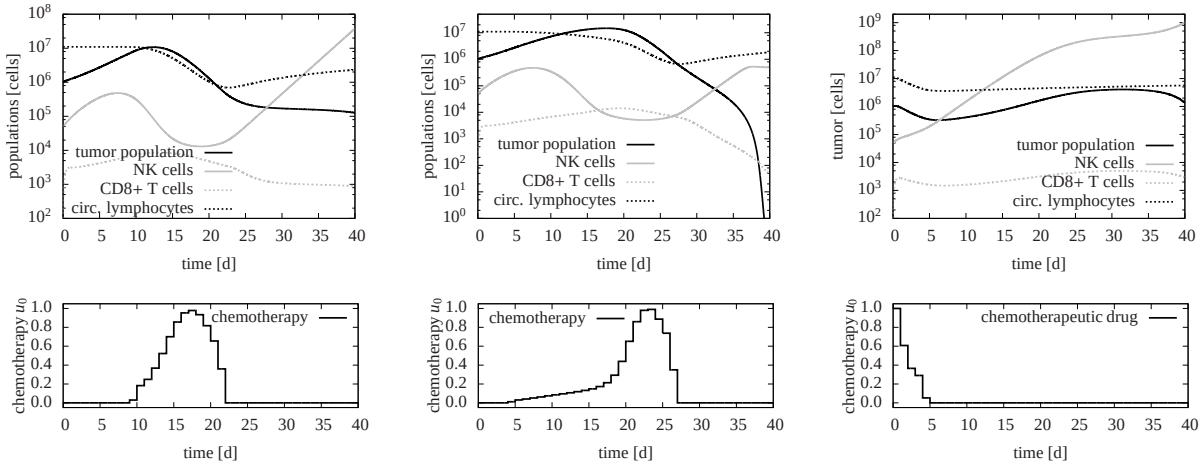

Figure 6: Optimization results for *de Pillis et al. (2006), mouse*, scenario (T1). Upper row: differential states, the tumor population $x_0(\cdot)$ in dark. Lower row: chemotherapy control. Left: weighted sum objective (O3) as in Figure 5 left. Middle: the same scenario under minimization of the tumor at the end time and a penalty on chemotherapy, (O5). Right: The plot shows a different local minimum, objective (O3) as in the left plot. Note the lower *integrated* tumor volume in the left and right plots, at the price of not eliminating the tumor at the end time.

minimal average value (e.g., minimizing tumor invasiveness and destruction of surrounding tissue) should be important and will depend on the type of tumor, its location in the body and its absolute initial size.

The influence of the immunotherapy in the *de Pillis* models was surprisingly low. As the results are not fully convincing from a practical point of view in our opinion, further efforts should be devoted to a more detailed modeling of the interplay between immune system and cancer growth and its quantitative understanding.

Generally, only few data are available for parameter sets, particularly in the case of human models, and obviously there is a significant variation from cancer type to cancer type and even from patient to patient. Therefore, we are aware that our current solutions are of no practical relevance for clinical applications, but they provide a proof of principles of what could be possible. It is obvious that an intense interdisciplinary cooperation between mathematicians, biologists, and physicians will be necessary to bridge this gap and to bring optimal control techniques into medical practice.

Acknowledgements

Financial support of the Heidelberg Graduate School of Mathematical and Computational Methods for the Sciences is gratefully acknowledged. Special thanks go to Georg Bock and Johannes Schlöder for providing the optimal control software package MUSCOD-II. DL thanks FRISYS, the Freiburg part of FORSYS initiative of the German Bundesministerium für Bildung und Forschung for support.

[1] F. Lévi, A. Okyar, S. Dulong, P. Innominato, J. Clairambault, Circadian timing in cancer treatments, Annual Review of Pharmacology and Toxicology 50 (2010) 377–421.

[2] J. Clairambault, Modelling physiological and pharmacological control on cell proliferation to optimise cancer treatments, Mathematical Modelling of Natural Phenomena 4 (3) (2009) 12–67.

[3] L. de Pillis, W. Gu, A. Radunskaya, Mixed immunotherapy and chemotherapy of tumors: modeling, applications and biological interpretations, Journal of Theoretical Biology 238 (4) (2006) 841–862.
URL http://www.sciencedirect.com/science/article/B6WMD-4H2G0D7-

[4] M. E. Dudley, J. R. Wunderlich, P. F. Robbins, J. C. Yang, P. Hwu, D. J. Schwartzentruber, S. L. Topalian, R. Sherry, N. P. Restifo, A. M. Hubicki, M. R. Robinson, M. Raffeld, P. Duray, C. A. Seipp, L. Rogers-Freezer, K. E. Morton, S. A. Mavroukakis, D. E. White, S. A. Rosenberg, Cancer regression and autoimmunity in patients after clonal repopulation with antitumor lymphocytes, Science 298 (2002) 850–854.

[5] P. Hahnfeldt, D. Panigraphy, J. Folkman, L. Hlatky, Tumor development under angiogenic signaling: A dynamical theory of tumor growth, treatment response, and postvascular dormancy, Cancer Research 59 (1999) 4770 – 4775.

[6] A. Ergun, K. Camphausen, L. M. Wein, Optimal scheduling of radiotherapy and angiogenic inhibitors, Bulletin of Mathematical Biology 65 (2003) 407–424.

[7] A. d'Onofrio, U. Ledzewicz, H. Maurer, H. Schaettler, On optimal delivery of combination therapy for tumors, Mathematical Biosciences 222 (2009) 13–26.

[8] L. de Pillis, A. Radunskaya, A mathematical tumor model with immune resistance and drug therapy: an optimal control approach, Journal of Theoretical Medicine 3 (2001) 79–100.

[9] L. de Pillis, K. Fister, W. Gu, T. Head, K. Maples, T. Neal, A. Murugan, K. Kozai, Optimal control of mixed immunotherapy and chemotherapy of tumors, Journal of Biological Systems 16 (1) (2008) 51–80.

[10] S. Chareyron, M. Alamir, Mixed immunotherapy and

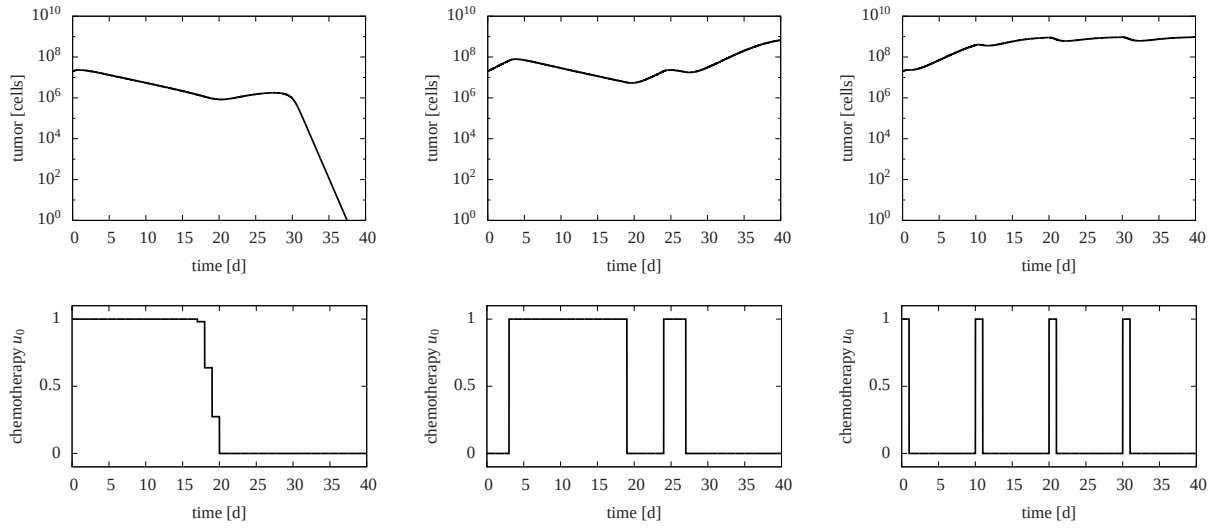

Figure 7: Optimization results for *de Pillis et al. (2006), human 9*, scenario (T4). Upper row: tumor population. Lower row: chemotherapy control u_0. Left: minimization of tumor at end time with penalty on chemotherapy control (O5). Middle: maximization, objective (O6). Right: standard therapy (example from [3]). Immunotherapy is (almost) zero in all cases. The optimal treatment makes the difference between a completely diminishing and a growing tumor here.

chemotherapy of tumors: Feedback design and model updating schemes, Journal of Theoretical Biology 45 (2009) 1052–1057.

[11] O. Isaeva, V. Osipov, Different strategies for cancer treatment: mathematical modeling, Computational and Mathematical Methods in Medicine 10 (2009) 253 – 272.

[12] A. d'Onofrio, A. Gandolfi, Tumour eradication by antiangiogenic therapy: analysis and extensions of the model by Hahnfeldt et al., Mathematical Biosciences 191 (2004) 159–184.

[13] A. d'Onofrio, A. Gandolfi, The response to antiangiogenic anticancer drugs that inhibit endothelial cell proliferation, Applied Mathematics and Computation 181 (2006) 1155–1162.

[14] J. Folkman, Anti-angiogenesis: New concept for therapy of solid tumors, Annals of Surgery 175 (1972) 409–416.

[15] L. de Pillis, A. Radunskaya, The dynamics of an optimally controlled tumor model: A case study, Mathematical and Computer Modelling 37 (2003) 1221–1244.

[16] L. G. de Pillis, A. E. Radunskaya, C. L. Wiseman, A validated mathematical model of cell-mediated immune response to tumor growth, Cancer Research 65 (2005) 7950–7958.

[17] A. Diefenbach, E. R. Jensen, A. M. Jamieson, D. H. Raulet, Rae1 and H60 ligands of the NKG2D receptor stimulate tumour immunity, Nature 413 (2001) 165–171.

[18] V. A. Kuznetsov, I. A. Makalkin, M. A. Taylor, A. S. Perelson, Nonlinear dynamics of immunogenic tumors: Parameter estimation and global bifurcation analysis, Bulletin of Mathematical Biology 56 (1994) 295–321.

[19] D. Kirschner, J. C. Panetta, Modeling immunotherapy of the tumor - immune interaction, Journal of Mathematical Biology 37 (1998) 235–252.

[20] U. Ledzewicz, H. Maurer, H. Schättler, Bang-bang and singular controls in a mathematical model for combined anti-angiogenic and chemotherapy treatments, in: Proceedings of the 48th IEEE Conference on Decision and Control, 2009.

[21] M. Engelhart, Modeling, simulation, and optimization of cancer chemotherapies, Diploma thesis, Heidelberg University (2009).
URL http://mathopt.uni-hd.de/PUBLICATIONS/Engelhart2009.pdf

[22] H. Bock, K. Plitt, A Multiple Shooting algorithm for direct solution of optimal control problems, in: Proceedings of the 9th IFAC World Congress, Pergamon Press, Budapest, 1984, pp. 243–247, available at http://www.iwr.uni-heidelberg.de/groups/agbock/FILES/Bock1984.pdf.
URL http://www.iwr.uni-heidelberg.de/groups/agbock/FILES/Bock19

[23] D. Leineweber, I. Bauer, H. Bock, J. Schlöder, An efficient multiple shooting based reduced SQP strategy for large-scale dynamic process optimization. Part I: Theoretical aspects, Computers and Chemical Engineering 27 (2003) 157–166.

[24] J. Betts, Practical Methods for Optimal Control Using Nonlinear Programming, SIAM, Philadelphia, 2001.

[25] C. Büskens, H. Maurer, Sqp-methods for solving optimal control problems with control and state constraints: adjoint variables, sensitivity analysis and real-time control, Journal of Computational and Applied Mathematics 120 (2000) 85–108.

[26] C. Büskens, H. Maurer, Sensitivity Analysis and Real-Time Control of Parametric Optimal Control Problems Using Nonlinear Programming Methods, Springer-Verlag, 2001, Ch. 1, pp. 57–68.

[27] H. Maurer, C. Büskens, J. Kim, Y. Kaya, Optimization methods for the verification of second-order sufficient conditions for bang-bang controls, Optimal Control Methods and Applications 26 (2005) 129–156.
URL http://arachne.uni-muenster.de:8000/num/Arbeitsgruppen/ag_m

[28] R. Fourer, D. Gay, B. Kernighan, AMPL: A Modeling Language for Mathematical Programming, Duxbury Press, 2002.

[29] A. Wächter, L. Biegler, On the implementation of an interior-point filter line-search algorithm for large-scale nonlinear programming, Mathematical Programming 106 (1) (2006) 25–57.
URL http://www.research.ibm.com/people/a/andreasw/papers/ipopt.

[30] I. Bauer, Numerische Verfahren zur Lösung von Anfangswertaufgaben und zur Generierung von ersten und zweiten Ableitungen mit Anwendungen bei Optimierungsaufgaben in Chemie und Verfahrenstechnik, Ph.D. thesis, Universität Heidelberg (1999).
URL http://www.ub.uni-heidelberg.de/archiv/1513

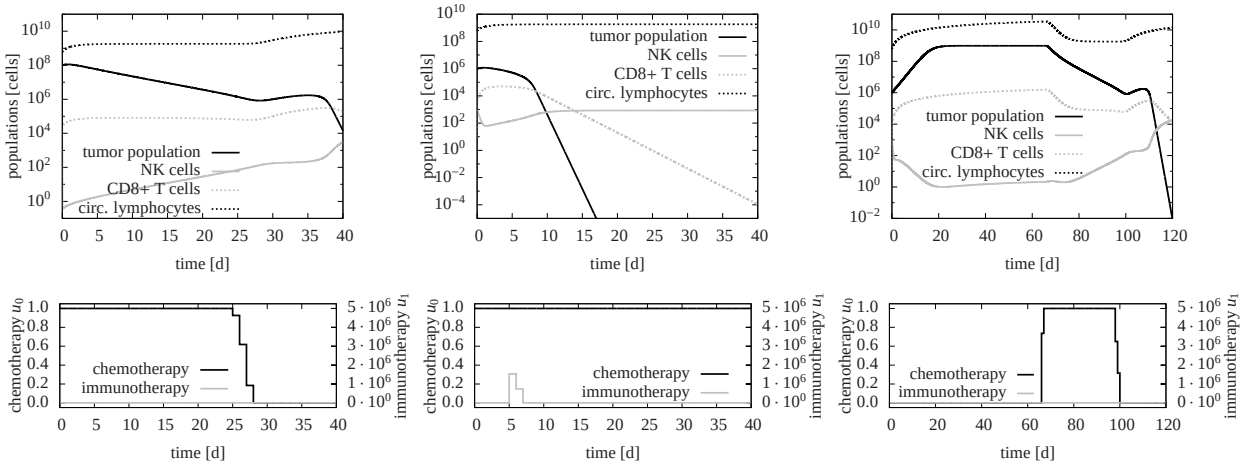

Figure 8: Optimization results for *de Pillis et al. (2006), human 9.* Upper row shows states, lower row controls. Left: scenario (T4) under weighted sum objective (O3) with end time $t_f = 40$ days – almost bang-bang solution. Center: scenario (T3) with end time $t_f = 40$ days under minimization of tumor at end time (O1) – full-dose solution with some immunotherapy. Note that there was no penalty on immunotherapy. Right: scenario (T3) with end time $t_f = 120$ days under minimization of tumor at end time with penalty on chemotherapy (O5).

[31] R. Wilson, A simplicial algorithm for concave programming, Ph.D. thesis, Harvard University (1963).

[32] M. Powell, A fast algorithm for nonlinearly constrained optimization calculations, in: G. Watson (Ed.), Numerical Analysis, Dundee 1977, Vol. 630 of Lecture Notes in Mathematics, Springer, Berlin, 1978.

[33] J. Nocedal, S. Wright, Numerical Optimization, 2nd Edition, Springer Verlag, Berlin Heidelberg New York, 2006, iSBN 0-387-30303-0 (hardcover).

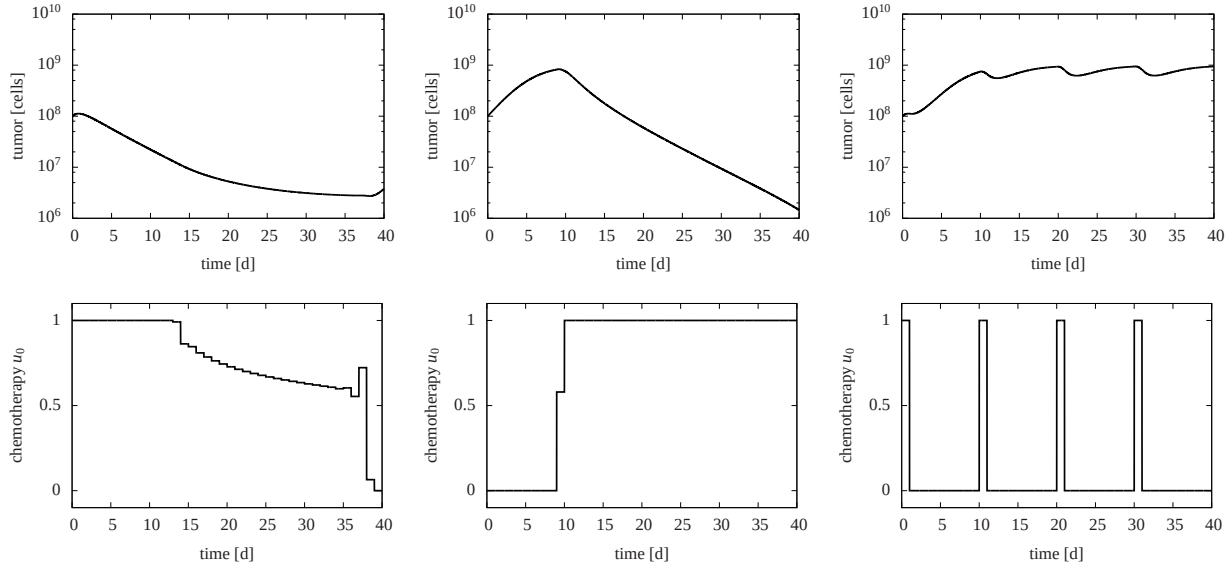

Figure 9: Optimization results for *de Pillis et al. (2006), human 10*, scenario (T5). Upper row: tumor population. Lower row: chemotherapy control u_0. Left: minimization of weighted sum (O3). Middle: maximization, objective (O4). Right: standard therapy (example from [3]). Immunotherapy is (almost) zero in all cases. Minimization is even a little higher than maximization at the end time, but the objective contains the minimization of the tumor over the whole time here, where the minimization is significantly better. Standard treatment is about 3 orders of magnitude worse due to a significantly lower total amount of drugs.

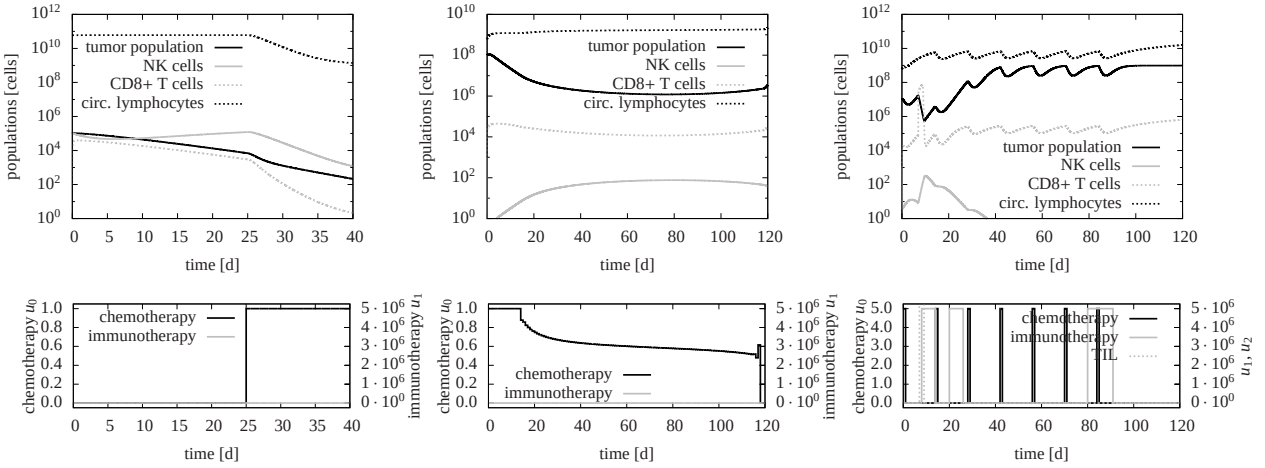

Figure 10: *de Pillis et al. (2006), human 10.* Left: Optimal control result for scenario (T7) with end time $t_f = 40$ days under minimization of tumor at the end time (O1). Center: optimal control result for scenario (T5) with end time $t_f = 120$ days under the weighted sum objective (O3). Right: Simulation of scenario (T6) with standard therapy including immunotherapy and TIL — the results from [3] could *not* be reproduced.

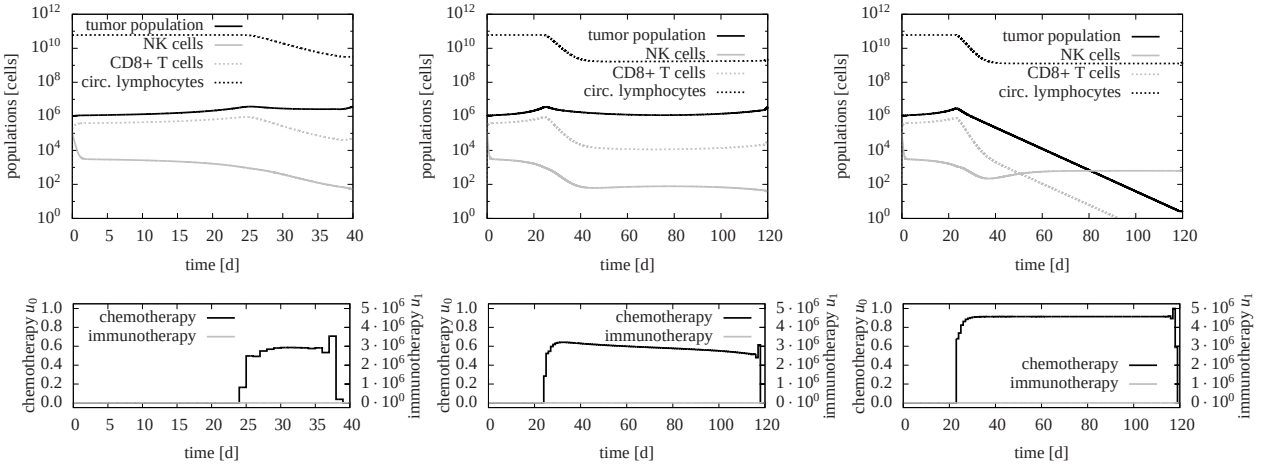

Figure 11: *de Pillis et al. (2006), human 10*, different optimal control results for scenario (T2). Upper row shows states, lower row controls. Left: Weighted sum objective (O3) with end time $t_f = 40$ days. Center: same objective (O3) with end time $t_f = 120$ days. Right: minimization of tumor at end time with penalty on chemotherapy (O5), end time at 120 days. In contrast to Figure 10 left, all solutions are dominated by singular arcs.